

An Additional Application of the Space Interferometry Mission to Gravitational Microlensing Experiments

Cheongho Han

Department of Astronomy & Space Science,
Chungbuk National University, Chongju, Korea 361-763
cheongho@astronomy.chungbuk.ac.kr

Tu-Whan Kim

Department of Astronomy,
Yonsei University, Seoul, Korea 120-749

Received _____; accepted _____

ABSTRACT

Despite the detection of a large number of gravitational microlensing events, the nature of Galactic dark matter remains very uncertain. This uncertainty is due to two major reasons: the lens parameter degeneracy in the measured Einstein timescale and the blending problem in dense field photometry. Recently, consideration has been given to routine astrometric followup observations of lensing events using the *Space Interferometry Mission* (SIM) as a means of breaking the lens parameter degeneracy in microlensing events. In this paper, we show that in addition to breaking the lens parameter degeneracy, SIM observations can also be used to correct for nearly all types of blending. Therefore, by resolving both the problems of the lens parameter degeneracy and blending, SIM observations of gravitational lensing events will significantly better constrain the nature of Galactic dark matter.

Subject headings: gravitational lensing – dark matter – astrometry – photometry

resubmitted to *Monthly Notices of the Royal Astronomy Society*: Dec. 28, 1998
Preprint: CNU-A&SS-09/98

1. Introduction

Surveys to detect Galactic dark matter by monitoring light variations of source stars caused by gravitational microlensing are being carried out by several groups and ~ 300 events have been detected (MACHO: Alcock et al. 1997a, 1997b; EROS: Ansari et al. 1996; OGLE: Udalski et al. 1997). The light curve of a lensing event is represented by

$$A_{\text{abs}} = \frac{u^2 + 2}{u(u^2 + 4)^{1/2}}; \quad u = \left[\beta^2 + \left(\frac{t - t_0}{t_E} \right)^2 \right]^{1/2}, \quad (1.1)$$

where the lensing parameters β , t_0 , and t_E represent the lens-source impact parameter, the time of maximum amplification, and the Einstein ring radius crossing time (Einstein timescale), respectively. Once the light curve of an event is observed, these lensing parameters are obtained by fitting the theoretical light curves of equation (1.1) to the observations. One can obtain information about individual lenses because the Einstein timescale is related to the physical lens parameters by

$$t_E = \frac{r_E}{v}, \quad r_E = \left(\frac{4GM}{c^2} \frac{D_{ol}D_{ls}}{D_{os}} \right)^{1/2}, \quad (1.2)$$

where r_E is the Einstein ring radius, v is the lens-source transverse speed, M is the lens mass, and D_{ol} , D_{ls} , and D_{os} are the separations between the observer, lens, and source star. However, since the Einstein timescale depends on a combination of the lens parameters, the values of the lens parameters determined from it suffer from large uncertainties.

The lens parameters suffer from additional uncertainties due to blending. The probability for a single source star to be in the state of gravitational amplification, i.e., the optical depth τ , is very low; from $(\mathcal{O})10^{-7}$ to $(\mathcal{O})10^{-6}$ depending on the observed field. To increase the event rate, therefore, experiments are being conducted toward very dense star fields such as the Galactic bulge and Magellanic Clouds. However, photometry of such dense star fields is affected by the flux from stars not participating in the gravitational lensing, the “blending problem.” Depending on the origin of the blended light, blending is classified into regular, amplification-bias, binary-source, and bright-lens blending (see § 2). When an event is affected by blending, the observed light curve is represented by

$$A_{\text{obs}} = A_{\text{abs}}(1 - f) + f; \quad f = \frac{B}{F_0 + B}, \quad (1.3)$$

where F_0 is the unblended flux of the source star before (or after) gravitational amplification, B is the amount of blended flux, and thus f represents the fraction of the blended light to the total observed flux. Therefore, when fitting a blended lensing event light curve, an additional lensing parameter f must be included. As a result, the determined lens parameters become even more uncertain.

Efforts to improve the results of gravitational microlensing experiments are therefore focused on breaking the lens parameter degeneracy and correcting for the blending effect.

Various methods have been proposed to do this. The methods for removing the degeneracy in the lens parameters are summarized by Jeong, Han, & Park (1999). Here we discuss the methods proposed to correct for various types of blending (see § 2). However, these methods are either applicable to only in a few rare cases or impractical due to the large uncertainty in the determined value of f . Therefore, to gain improved results from the next generation of lensing experiments, it is essential to devise practical methods that can resolve the problems of the lens parameter degeneracy and blending in general microlensing events.

Recently, routine astrometric followup observations of lensing events with high precision instruments such as the *Space Interferometry Mission* (hereafter SIM, Allen, Shao, & Peterson 1998) are being discussed as a method to break the lens parameter degeneracy of general microlensing events. When a source star is gravitationally lensed, it is split into two images. The image separation is too small for direct observation. However, the displacements of the light centroid of the two images can be measured with SIM. The trajectory of the centroid shifts is an ellipse (astrometric ellipse) whose shape depends on the lens-source impact parameter (see § 4.2). The usefulness of astrometric measurements of lensing events is that one can determine the angular Einstein ring radius, $\theta_E = r_E/D_{ol}$, from the measured centroid shifts because the size of the astrometric ellipse is directly proportional to θ_E . While the Einstein timescale depends on three lens parameters (M , D_{os} , and v), the angular Einstein ring radius depends only on two parameters (M and D_{ol}). Therefore, by measuring θ_E , the uncertainties in the determined lens parameters can be significantly reduced (Walker 1995; Paczyński 1998; Boden, Shao, & Van Buren 1998; Han & Chang 1998).

In this paper, we show that in addition to breaking the lens parameter degeneracy, observations with SIM can be used to correct for the blending effect in general microlensing events. Due to the high resolution, $\lesssim 0''.5$, from the diffraction-limited space observations, a significant fraction of events blended by field stars, i.e., regular and amplification-bias blended events, are automatically resolved by a single mirror of SIM. For events affected by very close blends with separations $\Delta\theta \lesssim 10$ mas, including a large fraction of binary companions and all bright lenses, one can also identify the lensed source star by detecting the distortions of the astrometric centroid trajectory caused by the blended star. For events affected by medium range separation blends, $10 \text{ mas} \lesssim \Delta\theta \lesssim 0''.5$, the blending effect can be corrected for by either detecting the shift of the broad envelope centroid between the point spread functions (PSFs) of lensed and blended stars caused by gravitational amplification or by examining the narrow fringe patterns observed at multi-wavelengths. Therefore, by resolving both the problems of lens parameter degeneracy and blending, SIM observations of gravitational lensing events will significantly better constrain the nature of Galactic dark matter.

2. Types of Blending

Depending on the origin of the blended light, blending is classified into several types. First, “regular blending” occurs when a star brighter than the detection limit, which is set by crowding, is lensed and the measured flux is affected by the residual flux from other blended stars fainter than the detection limit. Due to regular blending, the apparent amplification of the event is lower than its intrinsic value. As a result, the apparent Einstein timescale is shorter than its true value, resulting in systematic underestimation of lens masses (Di Stefano & Esin 1995; Woźniak & Paczyński 1997; Han 1998b). Since the optical depth is directly proportional to the timescale, the value of τ determined without properly correcting for regular blending is also underestimated.

The observed light curve is also affected by blending when one of several unresolved faint stars below the detection limit is lensed and its flux is associated with the flux from other field stars in the effective seeing disk of a monitored bright source star. This is known as “amplification-bias blending” (Bouquet 1993; Nemiroff 1994). The effects of amplification-bias blending for the determination of individual lens parameters are similar to those of regular blending, but the effects are more severe due to the much larger amount of blended light. However, the most important effect of amplification bias blending is that when not accounted for, the optical depth might be significantly overestimated (Alard 1997). This is because τ is determined based only on the number of monitored stars brighter than the detection limit, while events are actually detected among a larger number of stars, including fainter stars. Han (1997) estimated that the increase in τ caused by the miscount of effectively monitored stars is large enough to compensate the decrease in τ due to the decrease in timescales and make the observed optical depth overestimated by a factor ~ 1.7 .

In addition to background stars the lens itself can cause blending known as “bright lens blending” (Kamionkowski 1995; Buchalter & Kamionkowski 1997; Nemiroff 1997; Han 1998a). Bright lens blending causes the measured timescale and optical depth to be underestimated in the same manner as regular blending. In addition to the effects of regular blending, lens blending causes the determined optical depth to depend on the lens location. This is because detecting events caused by bright lenses close to the observer is comparatively more difficult than detecting events produced by lenses near the source. Additionally, since the brighter the lens is, the more massive it tends to be, and thus the more likely it is to be affected by lens blending. As a result, the decrease in optical depth for massive lenses is relatively bigger than the decrease for low-mass lenses, making the measured optical depth dependent on the lens mass function.

Finally, the last type of blending, known as “binary star blending” occurs when the source is a binary. In general, the typical separation between the component stars in a binary system is larger than the typical size of the Einstein ring radius. In this case only one star is significantly amplified, and the flux from the other star simply contributes as blended light (Dominik 1998). For some binaries with small component separations, on the

other hand, both component stars can be amplified. However, even in these cases it is not easy to detect the binarity of the source because the light curve mimics that of a single source event with a longer timescale and larger impact parameter than the true values (Griest & Hu 1992; Han & Jeong 1998).

3. Limitations of Current Blending-Correction Methods

There have been various methods proposed to correct for the blending problem. However, these methods are either applicable to only a few specific types of blending or impractical due to the large uncertainty in the determined value of f . In this section, we list these proposed methods and discuss their performance in correcting blending effects.

Because a blended event light curve is not exactly the same as that of an unblended event, ideally the effects are detectable using *photometry*. However, due to the limits on photometric precision of the current lensing experiments, blending has been photometrically detected only in a small number of events. Nevertheless, photometry is still being discussed because of the rapidly increasing photometric precision made possible through the operation of early warning systems (MACHO: Alcock et al. 1996; OGLE: Udalski et al. 1994) and subsequent effective followup observations (PLANET: Albrow et al. 1998; GMAN: Alcock et al. 1997c). However, we still find that even with this higher precision photometry, the uncertainties in the derived lensing parameters are very large, making it difficult to properly correct for blending effects. To demonstrate this, we simulate model events that are affected by various amounts of blended light and estimate the uncertainties of the recovered lensing parameters. The events are assumed to have $\beta = 0.3$, and $t_{E,0} = 15$ days, which are the most common values for the Galactic bulge events, and are affected by blending with various blended light fractions of $f = 0.3, 0.5, 0.7$, and 0.9 . The events are assumed to be observed 5 times/day during $-0.5t_E \leq t_{\text{obs}} \leq 3t_E$ with a high photometric precision of $p = 1\%$. The light curves are then fit with a theoretical blended light curve as given by equation (1.3). We estimate the uncertainties of the recovered lensing parameters by computing the values of χ^2 by

$$\chi^2 = \sum_{i=1}^{N_{\text{dat}}} \left(\frac{A_O - A_T}{pA_T} \right)^2, \quad (3.1)$$

where N_{dat} is the number of data points and A_O and A_T represent the simulated and theoretical model light curves, respectively. In Figure 1, we present the resulting values of χ^2 as functions of $t_E/t_{E,0}$ and f . The degrees of freedom are determined by $\text{dof} = N_{\text{dat}} - N_{\text{par}} - 1$, where $N_{\text{par}} = 4$ is the number of lensing parameters for the blended light curve fit. The contours are drawn at the levels of $\Delta\chi^2 = 1.0, 4.0$, and 9.0 (i.e., 1σ , 2σ , and 3σ levels) from inside to outside. From the figure, one finds that the uncertainties in both the derived values of t_E and f are large. One also finds that the uncertainty ranges of the blended light fraction measured at all levels include $f = 0$ (i.e.,

no blended light), implying that it will be difficult to detect blending effect even with high precision photometry. In addition, since the uncertainties increase rapidly with increasing values of f , correcting for blending effects using this method will be especially difficult for amplification-bias events which are severely affected by blending.

Another method of correcting for blending effects is to detect color shifts during an event with high precision, multi-band photometry (Buchalter, Kamionkowski, & Rich 1996). This method might be applicable if the lensed source star has a very different color from that of the integrated light of the blended stars. However, the expected amount of color shift is generally very small because most Galactic bulge stars have similar colors (Goldberg 1998). In addition, even when the color shift is detected, the determined lens parameters suffer from the same degeneracy as in the case of single-band photometry, making it difficult to properly correct for the blending effect (Woźniak & Paczyński 1997).

A more general method of correcting for blending effects is by detecting the shifts of a source star’s image centroid, δx , during an event (Alard, Mao, & Guibert 1995; Alard 1996). If one of many stars in a blended seeing disk is gravitationally amplified, the position of the center of light will shift toward the lensed star by an amount

$$\delta x = \eta |\langle \vec{x} \rangle - \vec{x}_0|; \quad \eta = \frac{A_{\text{obs}} - 1}{A_{\text{obs}}} = \frac{(1 - f)(A_{\text{abs}} - 1)}{A_{\text{abs}}(1 - f) + f}, \quad (3.2)$$

where $\langle \vec{x} \rangle$ is the position of the center of light before gravitational amplification and \vec{x}_0 is the location of the lensed star. Goldberg & Woźniak (1997) actually applied this method to the OGLE data base and found that 7 out of 15 tested events showed significant centroid shifts of $\delta x \gtrsim 0''.2$, demonstrating the usefulness of this method. However, not all blended events produce large centroid shifts. If the amplification of an event is very low, i.e., $A_{\text{abs}} \sim 1$, the expected centroid shift is small since $\eta \sim 0$. In addition, if the lensed star is the brightest one in the blended seeing disk and its flux dominates that from the other blended stars, the expected amount of centroid shift is very small even for a high amplification event because the position of the center of light before gravitational amplification will be very close to that of the lensed star, i.e., $|\langle \vec{x} \rangle - \vec{x}_0| \sim 0$. For large centroid shifts, therefore, the lensed star should be one of the faint stars in the seeing disk so that it has a negligible effect on the position of the center of light (Han, Jeong, & Kim 1998). For amplification-biased events, source stars are generally very faint. Because they are faint, the fact that they are detectable implies that the source stars are highly amplified. Since the conditions for detecting amplification-biased events agree well with those for large centroid shifts, the centroid shift measurement is an efficient method for detecting amplification-bias blending. However, this method is not efficient for detecting other types of blending. First, because of a relatively small amount of blended light, regular blended events do not need to be highly amplified to be detected. Although they can be highly amplified, the dominance of the source flux over that from other faint blended stars will result in small centroid shifts. This method is also inefficient for an event affected by the light from very closely located

blends such as binary companions and bright lenses due to the small amount of expected centroid shift.

4. Correction of Blending Effect by SIM

In the previous section, we showed that correcting for blending effects for general microlensing events is difficult by using the previously proposed methods. In this section we show that with diffraction-limited, single-mirror images and the high astrometric precision of SIM, one can correct for the effects of nearly all types of blending.

The optics of SIM can be modeled by a diffraction-limited telescope with two circular mirrors. Then the expected PSF is given by the classical double circular-aperture diffraction pattern formula of

$$I(\theta) = I_0 \left[\frac{2J_1(\pi\theta D/\lambda)}{\pi\theta D/\lambda} \right]^2 \cos^2 \left(\frac{\pi\theta d}{\lambda} \right), \quad (4.1)$$

where I_0 is the intensity of the central peak, d is the separation between the two mirrors with an aperture diameter D , λ is the observed wavelength, θ is the angle measured from the central fringe, and J_1 is the 1st-order Bessel function (Hecht 1998). According to the specification of SIM, $d = 10$ m and $D = 0.3$ m. The upper left two panels of Figure 2 show the expected PSF when a single (unblended) source star is observed by SIM. When observed at $\lambda \sim 5500$ Å, the PSF has a “broad envelope” of a width $1.22\lambda/D \sim 0''.5$ modulated by “narrow fringes” of a width $\lambda/d \sim 10$ mas.

When the source star is blended, however, the PSF takes a different form from that in equation (4.1). The blended source star PSF can be classified into three regimes depending on the separation $\Delta\theta$ between the lensed source and the blended star: regime 1 ($\Delta\theta \gtrsim 1.22\lambda/D$), regime 2 ($\Delta\theta < \lambda/d$), and regime 3 ($\lambda/d \leq \Delta\theta < 1.22\lambda/D$). In the following subsections, we investigate how the blends with various separations affect the PSF and their effects can be corrected for individual cases.

4.1. Regime 1 ($\Delta\theta \gtrsim 1.22\lambda/D \sim 0''.5$)

In this regime the broad envelopes of the two sources do not overlap (see the lower left panels of Figure 2), and thus the blended source is easily distinguished. In Baade’s Window the density of stars with $V < 23$, which are the major sources of blending, is less than 1 arcsec^{-2} according to the luminosity function determined from the *Hubble Space Telescope* observations by Holtzman et al. (1998). The stellar density in LMC field is even smaller. This implies that a significant fraction of sources blended by field stars, i.e., regular and amplification-bias blended events, are automatically resolved by a single mirror of SIM.

4.2. Regime 2 ($\Delta\theta < \lambda/d \sim 10$ mas)

In this case the narrow fringes from the two images overlap (the upper right panels of Figure 2). The position of the centroid of the central fringe, which is the position to be astrometrically measured by SIM, reflects the flux-weighted average of the two sources separately. Two classes of blending sources belong to this regime: a large fraction of binary companions to the source and all bright lenses. Of these two types of blending, Jeong, Han, & Park (1999) discussed in detail the effects of bright lenses on SIM observations and how to correct for blending effects caused by bright lenses. Here we focus on the effects of blending on events affected by binary star blending.

When a source star is gravitationally amplified, it is split into two images located on the same and opposite sides of the lens, respectively (see Figure 2 of Paczyński 1996). Due to the changes in position and amplification of the individual images caused by the lens-source transverse motion (see Figure 3 of Paczyński 1996), the light centroid between the images changes its location during the event. The location of the image centroid relative to the source star is related to the lensing parameters by

$$\delta\vec{\theta}_c = \frac{\theta_E}{u^2 + 2}(\mathcal{T}\hat{\mathbf{x}} + \beta\hat{\mathbf{y}}), \quad (4.2.1)$$

where $\mathcal{T} = (t - t_0)/t_E$ and $\hat{\mathbf{x}}$ and $\hat{\mathbf{y}}$ are the unit vectors toward the directions which are parallel and normal to the lens-source transverse motion, respectively. If we let $(x, y) = (\delta\theta_{c,x}, \delta\theta_{c,y} - b)$ and $b = \beta\theta_E/2(\beta^2 + 2)^{1/2}$, the coordinates are related by

$$x^2 + \frac{y^2}{q^2} = a^2, \quad (4.2.2)$$

where $a = \theta_E/2(\beta^2 + 2)^{1/2}$ and $q = b/a = \beta/(\beta^2 + 2)^{1/2}$. Therefore, during the event the trajectory of the source star image centroid traces out an astrometric ellipse (Walker 1995; Boden et al. 1998; Jeong et al. 1999).

However, when an event is affected by binary star blending, the centroid shift is affected by the light from the companion star and its trajectory deviates from an ellipse. Therefore, by detecting the distortion of the astrometric shift trajectory, it is possible to identify the blend and thus correct for the blending effect. In Figure 3, we illustrate the distortion of the astrometric shift trajectory when an event is blended by a binary companion with a light fraction of $f = 0.3$. In the figure, the dotted line represents the unperturbed trajectory of the centroid shift with respect to the position of the lensed source star located at the origin. As mentioned, the trajectory is an ellipse. On the other hand, when the event is blended by a companion star, located at $\delta\vec{\theta}_B$ with respect to the lensed star, the position of the light centroid will shift toward the companion. In addition, the reference position of the astrometric measurements is not the position of the lensed source star but the center of light between the binary components before amplification. Due to these two effects, the

resulting trajectory (represented by a solid line) of the astrometric shifts is no longer an ellipse. Note that since the majority of binaries in this regime have long orbital periods, for example $P \sim 30$ yrs for a Galactic bulge binary system with $\Delta\theta \sim 1$ mas, the motion of the blend is not important. Assuming that the distribution of separations for binaries in the solar neighborhood determined by Duquennoy & Mayor (1991) can be applied to bulge and LMC populations, $\gtrsim 60\%$ of Galactic and $\gtrsim 70\%$ of LMC binaries belong to this regime.

The trajectory of the centroid shift for a blended, binary event takes various forms depending on the fraction of blended light and the location of the blended star with respect to the lensed star. The centroid shift for an event blended by a binary companion is represented by

$$\vec{\delta\theta}_{c,\text{obs}} = \frac{1-f}{f+A_{\text{abs}}(1-f)} \left[A_{\text{abs}}\vec{\delta\theta}_c - f\vec{\delta\theta}_B(A_{\text{abs}}-1) \right]. \quad (4.2.3)$$

In the equation, the term including $\vec{\delta\theta}_c$ describes the elliptical motion of the centroid shift with respect to the lensed star (the elliptical term). On the other hand, the term including $\vec{\delta\theta}_B$ describes the linear shift caused by the light from the blended star (the linear term). Therefore, the shape of the astrometric shift trajectory for a blended event results from the combination of the elliptical displacement caused by gravitational lensing and the linear displacement toward the blended star. In Figure 4, we present various forms of the centroid shift trajectory as distorted by binary star blending. The left panels show how the trajectory changes from the unperturbed astrometric ellipse (in the top panel) with increasing fractions of blended light. To see the variation in the trajectory with respect to the location of the companion star, we also present the trajectories for various binary separations in the right panels.

4.3. (Regime 3 $\lambda/d \leq \Delta\theta < 1.22\lambda/D$)

In this case both the broad envelopes and fringes of the two PSFs are not matched (the lower right panels of Figure 1), and thus both centroids are shifted. The position of the centroid between the central broad envelopes is the flux-weighted average of the two sources and the amount of the shift is given by equation (3.2). One way to detect and correct for blending in this regime, therefore, is to measure the shift of the broad envelope centroid. However, the situation is slightly more complex for the position of the centroid of the narrow fringes. If the separation between two source is exactly the same as n times the width of the narrow fringe, i.e., $\Delta\theta = n\lambda/d$, the 0th fringe of the blend coincide exactly with the n th fringe of the lensed source. However, this is true only at a specific wavelength. If the blended source is observed at twice as long a wavelength, for example, the 0th fringe of the blend coincides exactly with the 1st null of the lensed source. Therefore, from the difference in the interference patterns observed at multiple wavelengths, one can deduce the position and brightness of the blend even if the observer chooses to examine the central

fringe rather than the whole interference pattern. The sources of blending belonging to this regime include large-separation binary companions to the lensed source and very closely located field stars.

5. Summary

By observing gravitational microlensing events with SIM, one can correct for the effects of nearly all types of blending. With its diffraction-limited, $\lesssim 0''.5$ imaging, a single mirror of SIM can resolve blended stars for a significant fraction of the events blended by field stars, such as regular and amplification-bias blended events. For events affected by very close blends with separations $\Delta\theta \lesssim 10$ mas, such as a large fraction of binary-star blended events, it is also possible to identify the blend by detecting a distortion in the astrometric shift trajectory. For events affected by blends with medium range separations, such as closely located field stars and wide binary companions, one can correct for the effects of blending by either detecting the shift of the broad envelope centroid between the PSFs of lensed and blended stars or by examining the narrow fringe patterns observed at multiple wavelengths.

We would like to thank to M. Everett and P. Martini for a careful reading of the manuscript. We also would like to thank the referee (A. Gould) for useful suggestions that improved the paper.

REFERENCES

- Alard, C. 1996, in IAU Symp. 173, *Astrophysical Applications of Gravitational Lensing*, ed. C. S. Kochanek & J. N. Hewitt (Dordrecht: Kluwer), 215
- Alard, C. 1997, *A&A*, 321, 424
- Alard, C., Mao, S., & Guibert, J. 1995, *A&A*, 300, L17
- Albrow, M., et al. 1998, *ApJ*, 509, 000
- Alcock, C., et al. 1996, *ApJ*, 463, L67
- Alcock, C., et al. 1997a, *ApJ*, 479, 119
- Alcock, C., et al. 1997b, *ApJ*, 486, 697
- Alcock, C., et al. 1997c, *ApJ*, 491, 436
- Allen, R., Shao, M., & Peterson, D. 1998, *Proc. SPIE*, 2871, 504
- Ansari, R., et al. 1996, *A&A*, 314, 94
- Boden, A. F., Shao, M., & Van Buren, D. 1998, *ApJ*, 502, 538
- Bouquet, A. 1993, *A&A*, 280, 1
- Buchalter, A., Kamionkowski, M., & Rich, M. R. 1996, *ApJ*, 469, 676
- Buchalter, A., & Kamionkowski, M. 1997, *ApJ*, 482, 782
- Di Stefano, R., & Esin, A. A. 1995, *ApJ*, 448, L1
- Dominik, M. 1998, *A&A*, 333, 893
- Duquenois, A., & Mayor, M. 1991, *A&A*, 248, 485
- Goldberg, D. M. 1998, *ApJ*, 489, 156
- Goldberg, D. M., & Woźniak, P. R. 1998, *Acta Astron.*, 48, 19
- Griest, K., & Hu, W. 1992, *ApJ*, 397, 362
- Han, C. 1997, *ApJ*, 484, 555
- Han, C. 1998a, *ApJ*, 500, 569
- Han, C. 1998b, *MNRAS*, submitted
- Han, C., & Chang, K. 1998, *MNRAS*, submitted
- Han, C., & Jeong, Y. 1998, *MNRAS*, 301, 231
- Han, C., Jeong, Y., & Kim, H.-I. 1998, *ApJ*, 507, 102
- Hecht, E. 1998, *Optics* (Reading: Addison-Wesley Longman), 461
- Holtzman, J. A., et al. 1998, *AJ*, 115, 1946
- Jeong, Y., Han, C., & Park, S.-H. 1999, *ApJ*, 511, 000

- Kamionkowski, M. 1995, *ApJ*, 442, L9
- Nemiroff, R. J. 1994, *ApJ*, 435, 682
- Nemiroff, R. J. 1997, *ApJ*, 486, 693
- Paczynski, B. 1996, *ARA&A*, 34, 419
- Paczynski, B. 1998, *ApJ*, 404, L23
- Udalski, A., et al. 1994, *Acta Astron.*, 44, 227
- Udalski, A., et al. 1997, *Acta Astron.*, 47, 169
- Walker, M. A. 1995, *ApJ*, 453, 37
- Woźniak, P., & Paczynski, B. 1997, *ApJ*, 487, 55.

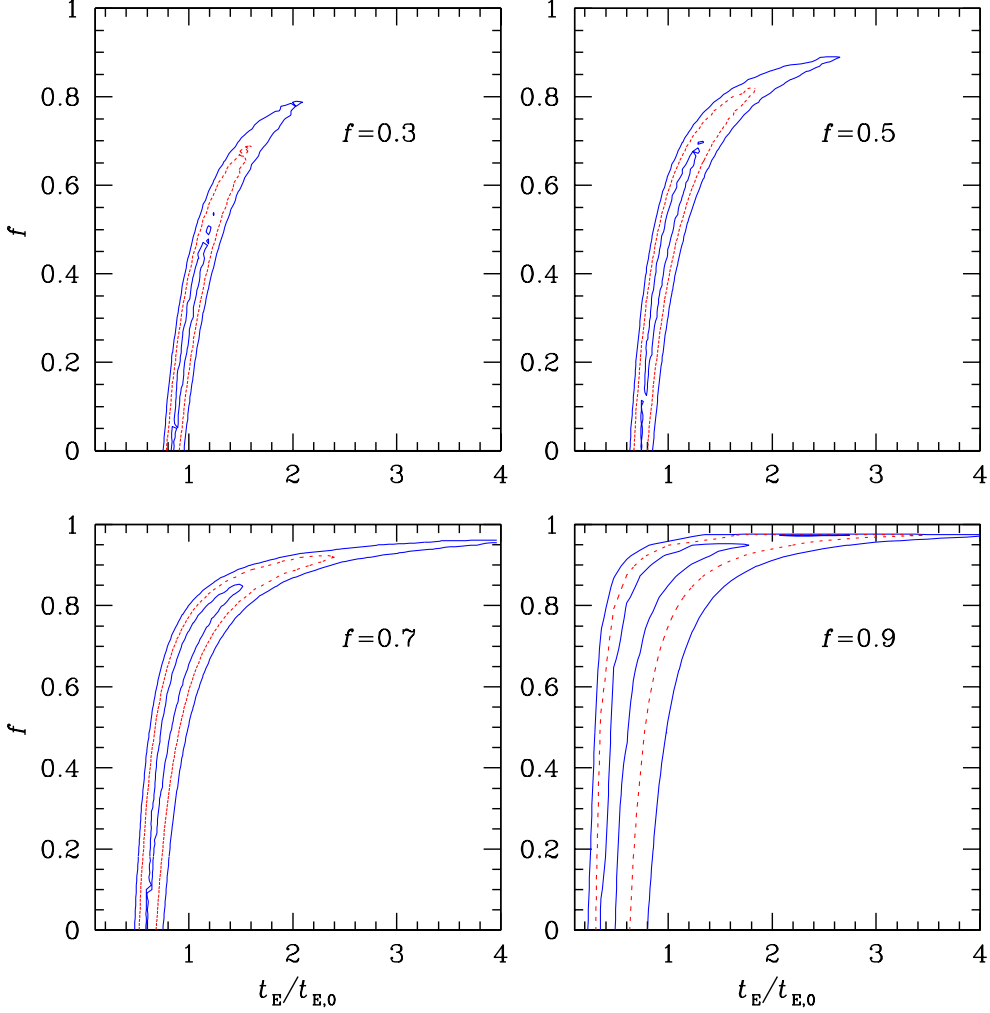


Figure 1: The uncertainties in the lensing parameters for events whose high precision light curves are fit with models. The events are assumed to have $t_E = 15$ days and $\beta = 0.3$, and are affected by blending with blended light fractions of $f = 0.3, 0.5, 0.7$, and 0.9 . The events are assumed to be observed 5 times/day during $-0.5t_E \leq t_{\text{obs}} \leq 3t_E$ with a photometric precision of $p = 1\%$. The uncertainties in the lensing parameters are determined by computing χ^2 , and the resulting χ^2 as functions of $t_E/t_{E,0}$ and f are presented as contour maps. In each panel, the contours are drawn at 1σ , 2σ , and 3σ levels from inside to outside.

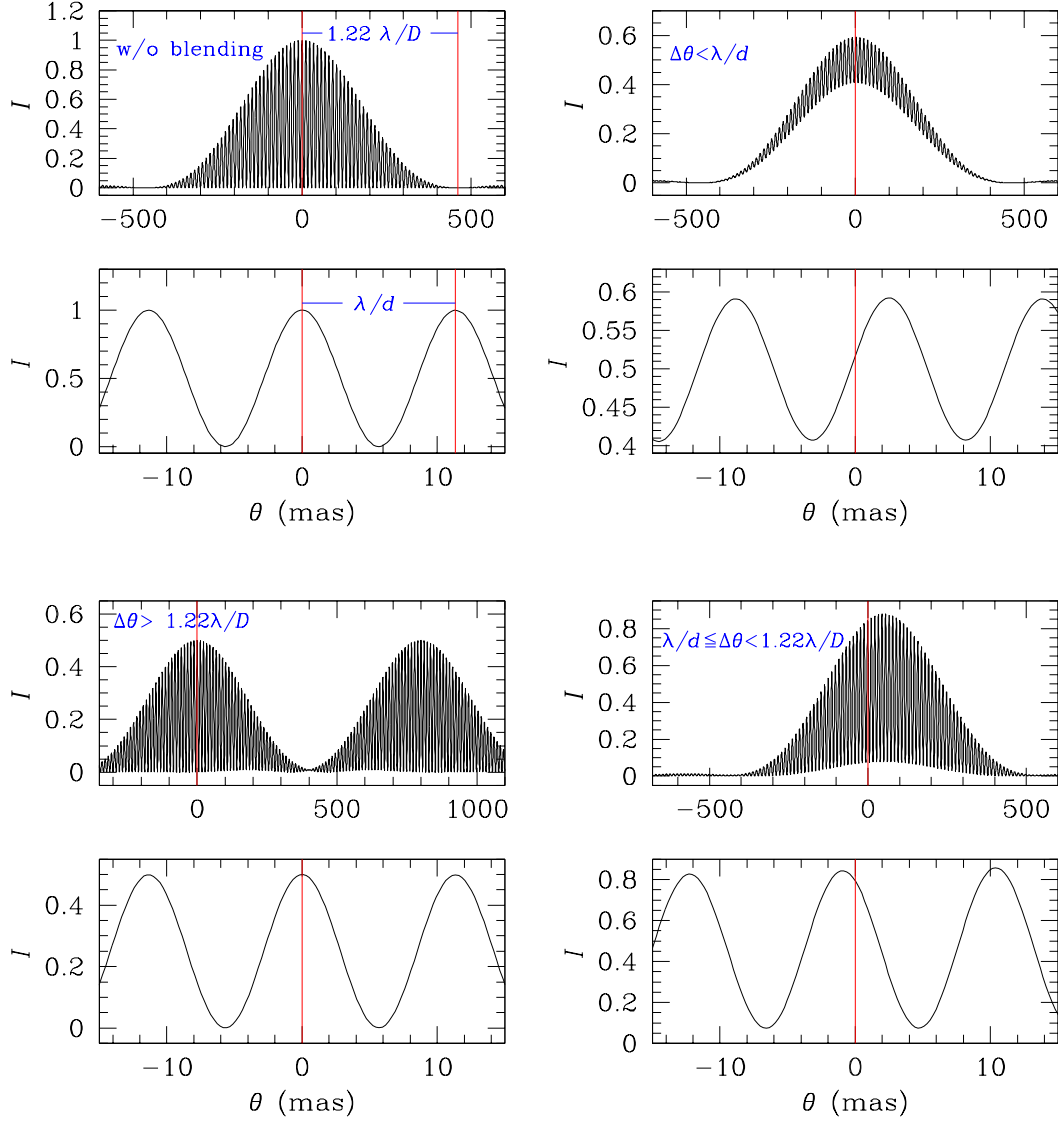


Figure 2: The expected fringe patterns when a source star affected by a blended star with various separations is observed by SIM. To better show the centroid shift of the narrow fringe pattern, the region around the position of the central fringe of the lensed star is expanded in the lower panel of each PSF. For all of these model events, we assume a blended light fraction of $f = 0.5$ and arbitrarily normalize the intensity.

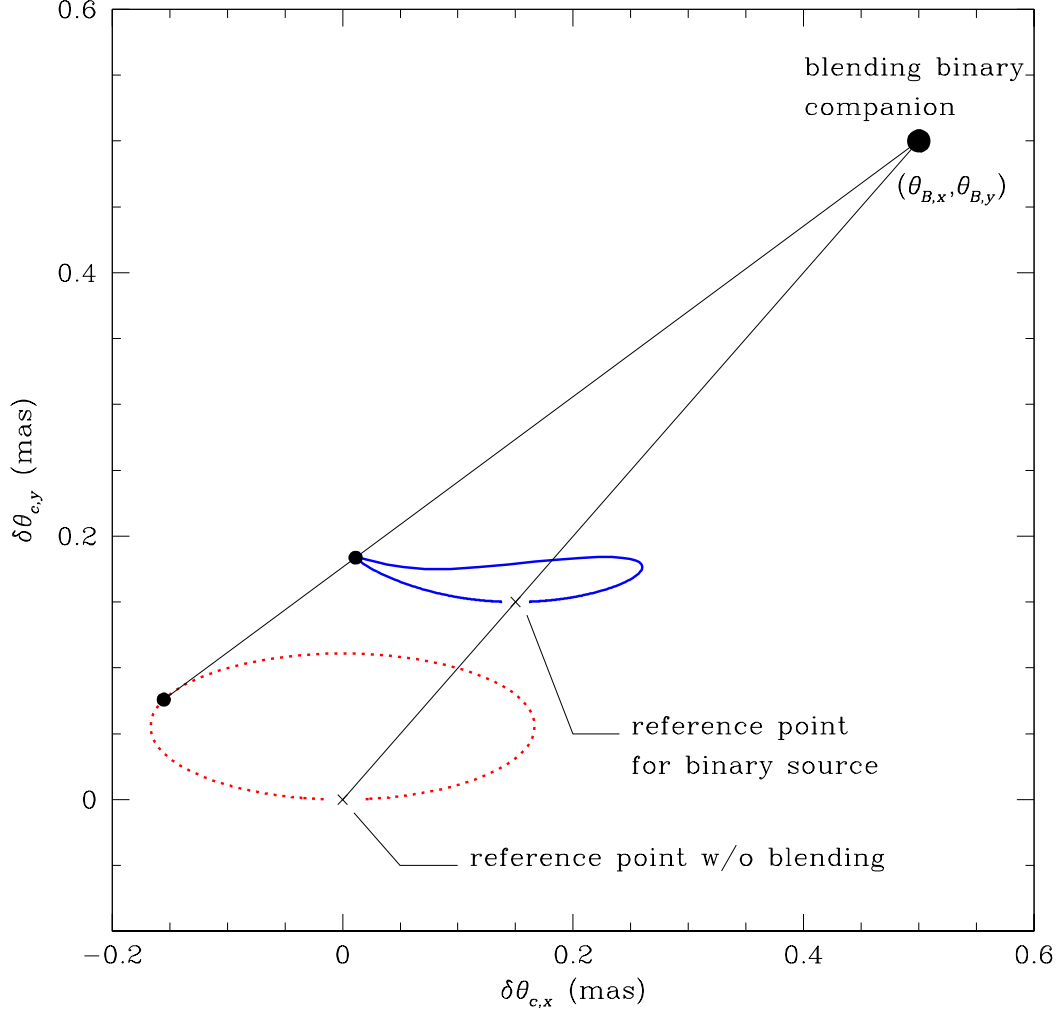


Figure 3: Illustration of the distortion of the astrometric shift trajectory by a binary companion. In the figure, the dotted line represents the trajectory of the centroid shifts with respect to the position of the source star located at the origin when the star is not affected by the binary-star blending. On the other hand, when the event is blended by a companion star, located at $(\theta_{B,x}, \theta_{B,y})$, the position of the light centroid will shift toward the companion. In addition, the reference position of the astrometric measurements is not the position of the lensed source star, but the center of light between the component stars. Due to these combined effects, the resulting trajectory (represented by a solid line) of the astrometric shifts is no longer an ellipse. This model event has lensing parameters of $t_E = 15$ days, $\theta_E = 0.5$ mas, and $\beta = 0.5$. The light fraction of the blended star is $f = 0.3$.

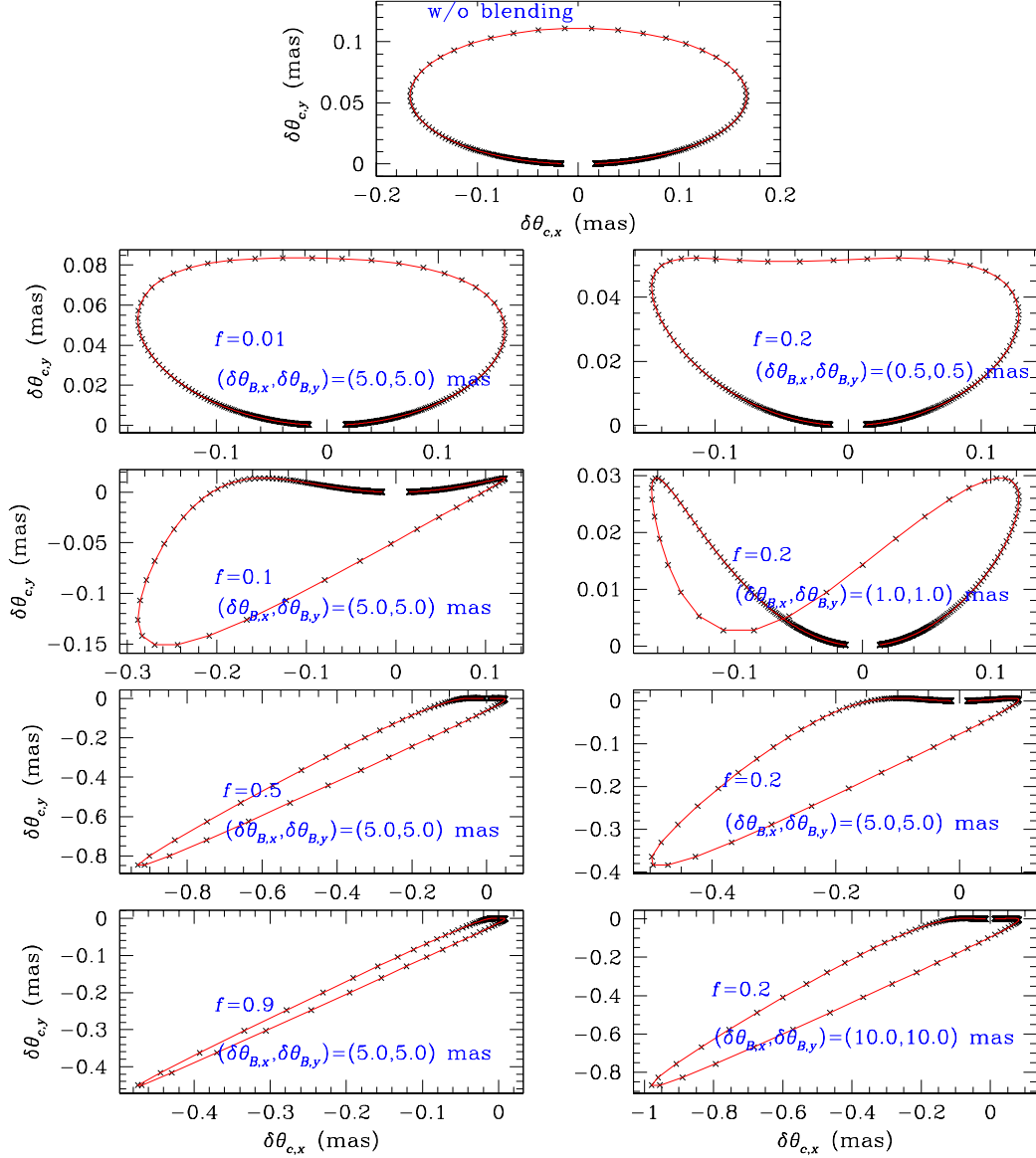


Figure 4: Various forms of the centroid shift trajectory distorted by binary-star blending. The left-side panels show how the trajectory changes from the unperturbed astrometric ellipse (in the top panel) with increasing fractions of blended light. To see the variation of the trajectory with respect to the location of the companion star, we also show the trajectories for various binary separations in the right-hand panels. This model event has lensing parameters of $t_E = 15$ days, $\theta_E = 0.5$ mas, and $\beta = 0.5$.